

## ANGIOTENSIN (5–8) MODULATES NOCICEPTION AT THE RAT PERIAQUEDUCTAL GRAY VIA THE NO–sGC PATHWAY AND AN ENDOGENOUS OPIOID

L. M. GUETHE,<sup>a,d</sup> A. PELEGRINI-DA-SILVA,<sup>c</sup>  
K. G. BORELLI,<sup>b,d</sup> M. A. JULIANO,<sup>e</sup> G. G. PELOSI,<sup>c,h</sup>  
J. B. PESQUERO,<sup>e</sup> C. L. M. SILVA,<sup>f</sup> F. M. A. CORRÊA,<sup>c</sup>  
F. MURAD,<sup>g</sup> W. A. PRADO<sup>c</sup> AND A. R. MARTINS<sup>c,d,\*</sup>

<sup>a</sup> Department of Psychology, FFCLRP University of São Paulo, Ribeirão Preto 14049-901, SP, Brazil

<sup>b</sup> Institute for Neurosciences and Behavior (INeC), University of São Paulo, Ribeirão Preto 14049-901, SP, Brazil

<sup>c</sup> Department of Pharmacology, School of Medicine of Ribeirão Preto, University of São Paulo, Ribeirão Preto 14049-900, SP, Brazil

<sup>d</sup> Institute of Biological Sciences, Federal University of Triângulo Mineiro, Uberaba 38025-015, MG, Brazil

<sup>e</sup> Department of Biophysics, Escola Paulista de Medicina-UNIFESP, São Paulo 04044-020, SP, Brazil

<sup>f</sup> Cellular and Molecular Pharmacology Research Program, ICB, Federal University of Rio de Janeiro, Rio de Janeiro 21941-599, RJ, Brazil

<sup>g</sup> Department of Biochemistry and Molecular Biology, George Washington University, Washington, DC 20037, USA

<sup>h</sup> Department of Physiological Sciences, Center of Biological Sciences, State University of Londrina, Londrina 86055-900, PR, Brazil

**Abstract—**Angiotensins (Angs) modulate blood pressure, hydro-electrolyte composition, and antinociception. Although Ang (5–8) has generally been considered to be inactive, we show here that Ang (5–8) was the smallest Ang to elicit dose-dependent responses and receptor-mediated antinociception in the rat ventrolateral periaqueductal gray matter (vlPAG). Ang (5–8) antinociception seems to be selective, because it did not alter blood pressure or act on vascular or intestinal smooth muscle cells. The non-selective Ang-receptor (Ang-R) antagonist saralasin blocked Ang (5–8) antinociception, but selective antagonists of Ang-R types I, II, IV, and Mas did not, suggesting that Ang (5–8) may act via an unknown receptor. Endopeptidase EP 24.11 and amastatin-sensitive aminopeptidase from the vlPAG catalyzed the synthesis (from Ang II or Ang III) and inactivation of Ang (5–8), respectively. Selective inhibitors of neuronal-nitric oxide

(NO) synthase, soluble guanylyl cyclase (sGC) and a non-selective opioid receptor (opioid-R) inhibitor blocked Ang (5–8)-induced antinociception. In conclusion, Ang (5–8) is a new member of the Ang family that selectively and strongly modulates antinociception via NO–sGC and endogenous opioid in the vlPAG. © 2012 IBRO. Published by Elsevier Ltd. All rights reserved.

**Key words:** angiotensin (5–8), antinociception, pain, periaqueductal gray matter, incision allodynia model, tail-flick test.

### INTRODUCTION

The brain renin–angiotensin (Ang) system (RAS) participates in cardiovascular and body fluid homeostasis and in neuronal plasticity (Antunes-Rodrigues et al., 2004; von Bohlen und Halbach and Albrecht, 2006; Bader, 2010). The brain RAS can also be involved in metabolic disorders and obesity (Baltatu et al., 2011) as well as in Alzheimer's disease (Wright and Harding, 2010). Evidence for the participation of the RAS in nociception has been based on the administration of Angs II, III and Ang receptor (Ang-R) antagonists into brain ventricles or medullary nuclei (Haulica et al., 1986; Shimamura et al., 1987; Yang et al., 1996; Georgieva and Georgiev, 1999; Marques-Lopes et al., 2009).

Prado et al. (2003) identified the ventrolateral periaqueductal gray matter (vlPAG) as a mesencephalic region where the injection of the tetradecapeptide renin substrate, Angs I, II and III, elicited antinociception in the rat tail-flick model. The injection of Ang II or Ang III into the vlPAG elicits Ang type 1 (AT<sub>1</sub>) and type 2 (AT<sub>2</sub>) receptor (R)-mediated antinociception that was detected using the tail-flick test. Both Losartan and CGP 42,112A, which are specific AT<sub>1</sub>R and AT<sub>2</sub>R antagonists (De Gasparo et al., 2000), respectively, blocked the antinociceptive activity (AA) of Ang II and Ang III injected into the vlPAG (Pelegrini-da-Silva et al., 2005, 2009). Each of these antagonists elicits an increase of post-incision allodynia when injected alone into the rat vlPAG, indicating that Ang II and/or Ang III is an endogenous modulator of vlPAG-mediated antinociception. The AA elicited by the injection of Ang II into the vlPAG has been ascribed to a dominant effect of Ang III synthesized from Ang II (Pelegrini-da-Silva et al., 2009).

\*Correspondence to: A. R. Martins, Institute of Biological Sciences, Federal University of Triângulo Mineiro (UFTM), Praça Manoel Terra, 330 – Abadia, Uberaba 38025-015, MG, Brazil. Tel: +55-1681122411.

E-mail address: armartin@fmrp.usp.br (A. R. Martins).

**Abbreviations:** AA, antinociceptive activity; Angs, angiotensins; Ang-R, Ang receptor; ANOVA, analysis of variance; AT, Ang type; ATR, Ang type receptor; DMSO, dimethylsulfoxide; HR, heart rate; MAP, mean arterial pressure; nNOS, neuronal nitric oxide synthase; NO, nitric oxide; NPLA, N<sup>ω</sup>-propyl-L-arginine; ODQ, 1H-[1,2,4]oxadiazolo-[4,3-a]quinoxalin-1-one; opioid-R, opioid receptor; PBS, phosphate-buffered saline; RAS, renin–angiotensin system; sGC, soluble guanylyl cyclase; vlPAG, ventrolateral periaqueductal gray matter.

The vPAG can synthesize Ang III, Ang (1–7), Ang IV and Ang (1–4) from Ang II (Pelegri-da-Silva et al., 2009); however, except for Ang III, the AA of these Ang II derivatives is not yet known. Here, we report a screen for AA of Ang peptides carried out by injecting Ang peptides into the vPAG and testing antinociception using the tail-flick test. Among the antinociceptive Angs identified, we further investigated Ang (5–8), which has generally been considered to be inactive in biological systems tested to date, except for inhibiting cell proliferation and viability in lactosomatotrophic (GH3) cell culture (Ptasinska-Wnuk et al., 2012). The antinociceptive effect of Ang (5–8) was approached using the tail flick and incision allodynia models, combined with an HPLC time-course of Ang (5–8) metabolism, with and without peptidase, neuronal nitric oxide (nNO) synthase (nNOS) and soluble guanylyl cyclase (sGC) inhibitors, and antagonists of Ang-R and opioid receptor (opioid-R), to study its synthesis, inactivation and mechanism of antinociceptive effect. The selectivity of the antinociceptive effect of Ang (5–8) was studied by injecting Ang (5–8) into the vPAG or intravascularly in normotensive rats, and by observing its effects on the isolated rat aorta and guinea-pig ileum.

## EXPERIMENTAL PROCEDURES

### Materials

Angs II, III, IV, (4–8) and (5–8), saralasin, Losartan and CGP 42,112A, were from Peninsula Laboratories (San Carlos, CA, USA). Divalinal-Ang IV, phenylephrine, acetylcholine, propranolol, sodium nitroprusside and N<sup>o</sup>-nitro-L-arginine were from Sigma (St. Louis, MO, USA). N<sup>o</sup>-propyl-L-arginine (NPLA) and 1H-[1,2,4]oxadiazolo-[4,3-a]quinoxalin-1-one (ODQ) were from Tocris (Bristol, UK).

### Subjects

Male albino Wistar rats weighing 140–160 g or 240–260 g were used for antinociception or blood pressure studies, respectively. All experiments were conducted according to our Institutions' guidelines for the use of laboratory animals. All protocols involving experiments with animals were approved by the Ethics Committees of the Federal University of Triângulo Mineiro (CEUA No. 181/2010), the Federal University of Rio de Janeiro (CEUA No. DFBCICB 011), and the Faculty of Medicine of Ribeirão Preto USP (CEUA No. 5.1.1209.53.8).

### Surgery

Rats were anesthetized with tribromoethanol (Sigma), 250 mg/kg body weight i.p. A 12-mm length of a 23-gauge stainless steel guide cannula was implanted into the skull to lie 3.0 mm above the target site in the PAG. The stereotaxic coordinates (in mm) used were the following: AP, 0.7 from the ear bars; L, 0.5 from the midline; and H, –3.1 from the skull surface, all taken from Paxinos and Watson's (1986) Atlas. The guide cannula was then fixed to the skull with two steel screws and dental cement. After receiving penicillin (50 mg/kg i.m.), the animal was allowed to recover for 5–7 days before the experiment. Intracerebral injection was carried out according to Azami et al. (1980). The volume injected was 0.25  $\mu$ L for all rats, delivered at a constant rate over a period of 40 s. The localization of the injection site was performed according to Pelegri-da-Silva et al. (2005).

I.c.v. injection was carried out using a stainless steel guide cannula of 0.7-mm outer diameter implanted into the lateral ventricle at the coordinates (in mm) AP = –1.5 from bregma, L = +1.8 from the medial suture, V = –2.9 from the skull and the incisive bar positioned at +2.5 mm from the interaural line. Two microliters of Ang II or Ang (5–8) in phosphate buffered saline (PBS) was injected using a 10  $\mu$ L syringe (705-N, Hamilton (Reno, Nevada, USA)) connected to a dental injection needle (200  $\mu$ m o.d.) by PE-10 tubing. The microinjection needle was 1 mm longer than the guide cannula.

### Tail-flick test

The rat was introduced into a glass tube for up to 20 s, with the tail laid across a nichrome wire coil at room temperature (23  $\pm$  2  $^{\circ}$ C). The coil temperature was then raised by an electric current until a tail withdrawal reflex occurred within 2.5–3.5 s. A cutoff time of 6 s was used. Tail-flick latencies were measured at 5-min intervals until a stable baseline was obtained over three consecutive trials (Pelegri-da-Silva et al., 2005). After baseline determination, antagonist, enzyme inhibitor (Losartan, CGP 42,112A, divalinal-Ang IV, compound A-779, NPLA, ODQ or naloxone) or vehicle was injected into vPAG, and tail-flick latencies were measured at 5-min intervals over 15 min. Five minutes later, vehicle or an Ang was injected intracerebrally and latencies were measured at 5-min intervals over a further 40-min period.

### Incision allodynia model

Rats were anesthetized with 1.5% halothane in oxygen. A 1-cm longitudinal incision was made with a surgical blade through the skin and fascia of the plantar region, starting 0.5 cm from the proximal edge of the heel (Pelegri-da-Silva et al., 2009). The plantaris muscle was elevated, but its origin and insertion were left intact. This procedure is similar to that reported by Brennan et al. (1996) and Vandermeulen and Brennan (2000). After hemostasis, the wound was sutured with two 5-0-nylon stitches. Rats were placed in an elevated clear plastic chamber with a wire mesh grid floor, which allowed easy access to the paw plantar surface. The threshold to mechanical stimulation was measured with an automated electronic von Frey apparatus (Digital Analgesimeter, Insight, Ribeirão Preto, SP, Brazil), consisting of a hand-held probe unit to which a rigid plastic tip (tip area 0.44 mm<sup>2</sup>) was connected. The experimenter applied the plastic tip with an increasing force in an upward direction against sites near the heel, 1–2 mm adjacent to the medial border of the wound. A single trial consisted of three applications of the stimulus, delivered at 10-s intervals. The mechanical threshold was tested 5 min before paw incision, 5 min before and after vehicle or Ang (5–8) (0.1, 0.2 and 0.4 nmol/0.25  $\mu$ L) injection into vPAG, and then at 5-min intervals for up to 50 min. The response was defined as withdrawal of the stimulated paw, followed by flinching movements.

### Arterial pressure and heart rate (HR) preparation

Male Wistar rats weighing 240–260 g were anesthetized with tribromoethanol (250 mg/kg i.p.). A polyethylene catheter was implanted into the left femoral artery for recording blood pressure. A similar catheter was introduced into the left femoral vein for intravenous drug injection or into carotid artery for intra-arterial administration in urethane-anesthetized rats and experiments were initiated 1 h after anesthesia onset. On the day of the experiment, the animals were allowed a 15-min period to adapt to the conditions of the experimental room, before starting blood pressure and HR recording. The experimental room was acoustically isolated and had constant

background noise generated by an air exhaust system. Care was taken to start the injections when HR and blood pressure were stable. The procedure to measure arterial pressure was the same for both anesthetized and freely moving animals. Mean arterial pressure (MAP) was recorded using an HP-7754A preamplifier (Hewlett Packard, USA) and an acquisition board (MP100A, Biopac Systems Inc., USA) connected to a computer. HR values were derived from the blood pressure recordings and processed online. Baseline blood pressure values were calculated as the average of the 1-min recording prior to the injection.

### Isolated guinea-pig ileum preparation

Guinea pigs weighing 200–250 g were starved for 24 h and killed by decapitation for mechanical recordings using isolated ileum preparations. A 20-cm portion of the terminal ileum was removed and washed at room temperature with Tyrode solution. Segments of 3-cm length were then cut and mounted in chambers containing 5 mL of Tyrode solution, maintained at 37 °C and bubbled with air (pH 8.4) or with a mixture of 95% O<sub>2</sub> and 5% CO<sub>2</sub> (pH 7.4). The strips of guinea-pig ileum were stretched with a resting tension of 1 g. Changes in tension produced by the peptides were measured with isometric transducer F-60 (International Biomedical, Inc., Austin, TX, USA) and a potentiometric recorder (RB-102; ECB, São Paulo, Brazil).

### Isometric contraction of isolated rat aorta

Aortic rings (3 mm wide) were fixed to an organ bath chamber filled with physiological solution (composition in mM: NaCl 122, KCl 5, NaHCO<sub>3</sub> 15, glucose 11.5, MgCl<sub>2</sub> 1.25, CaCl<sub>2</sub> 1.25 and KH<sub>2</sub>PO<sub>4</sub> 1.25) bubbled with 95% O<sub>2</sub>/5% CO<sub>2</sub>, under a resting tension of 20 mN at 37 °C. The rings were equilibrated with physiological solution for 60 min. Rings were pre-contracted with 1 or 0.3 μM phenylephrine to study the effect of Ang (5–8) in the absence or in the presence of N<sup>G</sup>-nitro-L-arginine, respectively, to maintain the amplitude of contraction, which corresponded to approximately 80% of the maximal contraction observed in a cumulative dose–response curve for phenylephrine. Acetylcholine (1 μM) was added at the plateau of the tonic contraction to assess that relaxation was endothelium-dependent. Rings that relaxed at least 80% were deemed endothelium-intact and thus used in the experiments (Tamura et al., 2009). Aortic rings were then washed, and a second contraction was induced by 1 μM phenylephrine to stabilize the preparation. Afterward, the rings were washed and left to equilibrate for 1 h, and then a third contraction was induced with 1 μM phenylephrine in the presence of 10 μM propranolol. At the plateau of the tonic contraction, Ang (5–8) was added cumulatively (0.01–3 μM). Constitutive NOS activity was inhibited with N<sup>G</sup>-nitro-L-arginine (100 μM, 1 h). In this case, because aortic rings were more sensitive to a constrictor agonist, preparations were pre-contracted with 0.3 μM phenylephrine to induce a tension equivalent to that observed in the absence of N<sup>G</sup>-nitro-L-arginine. Each ring was stimulated with Ang (5–8) only once. The effect induced by Ang (5–8) was expressed as percentage of the contraction induced by 1 μM phenylephrine. Sodium nitroprusside (10<sup>-9</sup>–10<sup>-5</sup> M) was used as a positive control for the NO–cGMP pathway vascular relaxation. Tension was measured isometrically using a Grass Transducer (FT-03; Grass Technologies (West Warwick, RI, USA)), and data were acquired and analyzed using Chart 3.4.9 software (MacLab, USA). The maximal effect ( $E_{max}$ ), the mean effective concentration of the agonist ( $EC_{50}$ ) and its negative logarithm ( $pD_2$ ) were estimated by non-linear regression using the software GraphPad Prism 5.0 (GraphPad, San Diego, California, USA, [www.graphpad.com](http://www.graphpad.com)).

### Metabolism of Angs II, III and Ang (5–8) by the vIPAG

The animals were decapitated, and then the brains were immediately dissected out and frozen. Punches of 0.5-mm outer diameter and 0.3-mm internal diameter were taken from 0.3-mm-thick cryostat sections of the vIPAG (Palkovits and Browstein, 1983). Tissues were homogenized in 50 mM Tris–HCl buffer, pH 7.4, using a micro-homogenizer (Thomas; Swedesboro, NJ, USA).

The liquid chromatographic system used here consisted of a Constametric 4100 Solvent Delivery System, a SM4000 absorbance detector set at 214-nm wavelength (both from LDC Analytical), and a Rheodyne injector model 7161 fitted with a 100-μL loop. The detector output was collected using LCTalk software, version 2.03.02 (LDC Analytical, Richmond, CA, USA), with a 1 V full scale. The mobile phase preparation and the chromatographic conditions used in this work were as previously described (Pelegri-da-Silva et al., 2002).

### Protein determination

Proteins were determined by the method of Lowry et al. (1951), using bovine serum albumin as the standard.

### Statistical analysis

Latencies were plotted as the mean ± S.E.M. The time-course of the effects obtained in the experimental groups was analyzed by multivariate analysis of variance (MANOVA). The factors analyzed were treatment, time and treatment × time interactions. In the case of a significant difference between treatments and/or significant treatment × time interactions, one-way ANOVA followed by Duncan's test was performed for each time point. Area under the curve was calculated for each individual animal using the Prism version 5 software (GraphPad, San Diego, CA, USA), and the different experimental groups were analyzed by ANOVA followed by Tukey's test. The level of significance was set at  $p < 0.05$  in all cases. MAP and HR were presented as the mean ± S.E.M. and were analyzed using Student's *t*-test (unpaired) and one-way ANOVA (Prism, GraphPad, USA). Aorta relaxation data were plotted as the mean ± S.E.M. Data from isometric contraction assays were compared by unpaired Student's *t*-test. Statistical significance was set at  $p < 0.05$ .

## RESULTS

### Ang (5–8) was the smallest Ang peptide that elicited a dose–response antinociceptive effect upon injection into the rat vIPAG

A screen for AA of Ang peptides using the tail-flick test showed that Ang (5–8), Ang (4–8), Ang IV and Ang (1–7) were biologically active upon injection into the vIPAG (Table 1). Ang (1–4), Ile-His-Pro, His-Pro-Phe and His-Pro were not active, suggesting that Ang (5–8) is the smallest Ang peptide exhibiting AA.

Ang (5–8) injected into the vIPAG regions indicated in Fig. 1A elicited a significant antinociceptive effect on both the tail flick and incision allodynia models of antinociception. The latency of the tail-flick reflex increased for up to 25 min following injection (Fig. 1B). The dose (0.05–1.6 nmol/0.25 μL)–response curve presented an inverted U-shaped pattern. Ang (5–8)-elicited antinociception was then tested using a model of incision allodynia (Fig. 1C). The withdrawal reflex before incision of the hind paw was elicited by the application of approximately 45 g of force. The mean threshold

**Table 1.** Structure–antinociceptive activity (AA) relationship for a series of angiotensin-peptides

|           | Peptide structure  | AA |
|-----------|--|----|
| Ang II    | Asp <sup>1</sup> -Arg <sup>2</sup> -Val <sup>3</sup> -Tyr <sup>4</sup> -Ile <sup>5</sup> -His <sup>6</sup> -Pro <sup>7</sup> -Phe <sup>8</sup> | +  |
| Ang (1–7) | Asp <sup>1</sup> -Arg <sup>2</sup> -Val <sup>3</sup> -Tyr <sup>4</sup> -Ile <sup>5</sup> -His <sup>6</sup> -Pro <sup>7</sup>                   | +  |
| Ang (1–4) | Asp <sup>1</sup> -Arg <sup>2</sup> -Val <sup>3</sup> -Tyr <sup>4</sup>   | –  |
| Ang III   | Arg <sup>2</sup> -Val <sup>3</sup> -Tyr <sup>4</sup> -Ile <sup>5</sup> -His <sup>6</sup> -Pro <sup>7</sup> -Phe <sup>8</sup>                   | +  |
| Ang IV    | Val <sup>3</sup> -Tyr <sup>4</sup> -Ile <sup>5</sup> -His <sup>6</sup> -Pro <sup>7</sup> -Phe <sup>8</sup>                                     | +  |
| Ang (4–8) | Tyr <sup>4</sup> -Ile <sup>5</sup> -His <sup>6</sup> -Pro <sup>7</sup> -Phe <sup>8</sup>   | +  |
| Ang (5–8) | Ile <sup>5</sup> -His <sup>6</sup> -Pro <sup>7</sup> -Phe <sup>8</sup>   | +  |
| Ang (5–7) | Ile <sup>5</sup> -His <sup>6</sup> -Pro <sup>7</sup>   | –  |
| Ang (6–8) | His <sup>6</sup> -Pro <sup>7</sup> -Phe <sup>8</sup>   | –  |
| Ang (6–7) | His <sup>6</sup> -Pro <sup>7</sup>   | –  |

The time-course of antinociception was detected by the tail-flick test for 40 min after injecting each peptide in 0.25 µL phosphate-buffered saline (PBS) or PBS alone (control, AA not elicited) into the rat vPAG, 1 min before starting the measurements (at zero time). +, indicates that a peptide exhibited AA, on the basis of differences ( $p < 0.05$ ) of latencies between peptide and PBS groups in the 0–40 min interval. –, indicates absence of detectable AA. Doses of peptides were 0.2 and 0.8 nmol for all of them. The number of rats per group was 6–9.

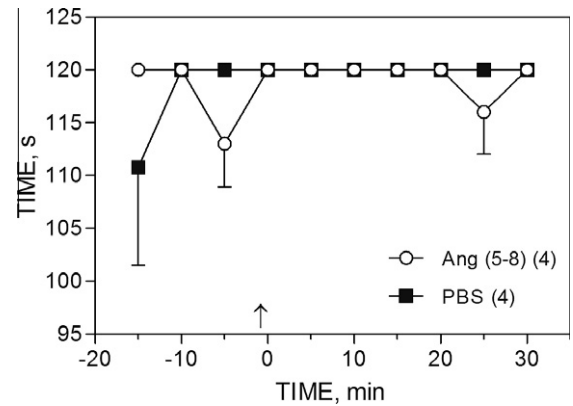


**Fig. 2.** The injection of Ang (5–8) into the vPAG did not change locomotor activity. Each rat was placed on the drum of a rota-rod apparatus (Ugo Basile, Comerio, Italy) rotating at 25 rpm for up to 2 min (cut-off time) and the latency to fall was recorded three times at 5-min intervals. Ang (5–8) or PBS was then injected into the vPAG and the animal was again positioned on the drum for a post-injection recording the latency to fall, which was then repeated at 5-min intervals for up to 30 min after the injection. Data are expressed as the mean ± S.E.M.

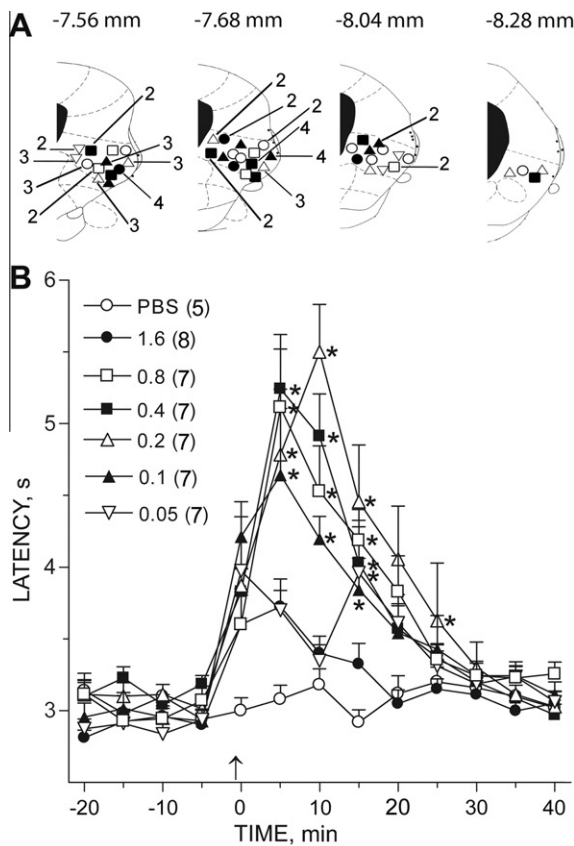


**Fig. 1.** Time-course of the antinociceptive effect of different doses of Ang (5–8) injected into the rat vPAG, detected using the tail-flick or incision allodynia models. (A) Coronal sections showing the location of injection sites into the PAG that lead to antinociception. (B) Tail-flick testing: Ang (5–8) or phosphate-buffered saline (PBS) was injected 1 min before (arrow) starting the measurements (at zero time) of tail-flick latencies. Doses of peptide (nmol) and number of rats (in parentheses) with their corresponding symbols are given on top of the graph. All injection volumes were 0.25 µL. Points represent means of latencies ± S.E.M. \*Different from the PBS group ( $p < 0.05$ ). (C) Incision allodynia testing: arrows 1 and 2 indicate the time of surgery, and the time of Ang (5–8) or PBS injection, respectively. The injection volume was 0.25 µL for all doses. Doses of Ang (5–8) (nmol) and number of rats (in parentheses) with their corresponding symbols are given on top of the graph. Points represent mean force applied on the paw ± S.E.M. \*Different from the PBS-treated group ( $p < 0.05$ ). (D) Coronal sections showing the location of Ang (5–8) injection sites that did not lead to antinociception.

measured at 5 min, *i.e.*, 2 h after surgery, decreased 55% from the upper limit of the test, thus characterizing the presence of incision allodynia. The injection of 0.1–0.4 nmol/0.25  $\mu$ L Ang (5–8) into the vIPAG produced a dose–response reduction of the incision allodynia that lasted for up to 25 min at the 0.2 nmol/0.25  $\mu$ L dose. The decrease of incision allodynia was maximal within the first 2–5 min after the 0.2 nmol/0.25  $\mu$ L dose, which elicited a significant 65% increase in the force required for paw withdrawal. The threshold of the non-incised hind paw did not change throughout the period of observation. The injection of Ang (5–8) into regions that were near to but outside the vIPAG (Fig. 1D) did not elicit any detectable antinociceptive response in the tail-flick or incision allodynia models, suggesting that this response was specifically elicited from the vIPAG. Moreover, the injection of Ang (5–8) into the vIPAG did not affect locomotor activity (Fig. 2). Thus, Ile-His-Pro-Phe, Ang (5–8), was the smallest Ang that elicited a region-specific and dose-dependent antinociceptive effect on both the tail flick and incision allodynia models, upon its injection into the vIPAG.

#### The antinociceptive effect of Ang (5–8) is Ang-R mediated, but is not blocked by selective antagonists of known Ang-Rs

Saralasin ([Sar<sup>1</sup>, Ala<sup>8</sup>]-Ang II) (1.0 nmol), a non-selective Ang-R antagonist, fully blocked the AA of 0.2 nmol/0.25  $\mu$ L Ang (5–8). Although saralasin can exhibit a partial agonist activity at high doses (De Gasparo et al., 2000), its injection alone into vIPAG had no detectable

effect on the tail-flick latency (Fig. 3A). However, the AA of Ang (5–8) was not inhibited by previous vIPAG injections of 25-pmol Losartan, 25-pmol CGP 42,112A, 0.1 and 1-nmol (not shown) divalinal-Ang IV or 0.3-nmol compound A-779, which are specific and selective antagonists of Ang-R types 1, 2, 4 (De Gasparo et al., 2000) and of Ang (1–7) acting via the Mas-R (Santos et al., 2003), respectively (Figs. 3B and 4A–D). None of the above antagonists alone led to a detectable change in the tail-flick latency upon injection into vIPAG (Fig. 4A–D). Thus, Ang (5–8) appears to mediate antinociception in the vIPAG through an unidentified Ang-R.

#### The vIPAG can synthesize and inactivate Ang (5–8)

The initial rate of hydrolysis of Ang II by a tissue homogenate from punches of the vIPAG was 1.03 nmol/min/mg protein, measured with 5-min incubation and corresponding to 12.9% Ang II hydrolysis. The complementary peptide products, Ang (1–4) and Ang (5–8), were formed in equimolar amounts after 5-min incubation (Fig. 5A), indicating the cleavage of the Tyr<sup>4</sup>-Ile<sup>5</sup> peptide bond in Ang II by an endopeptidase. The Tyr<sup>4</sup>-Ile<sup>5</sup> bond in Ang II can be cleaved by several endopeptidases, among them EP 24.11 (EC 3.4.24.11, neprilysin) (Almenoff and Orłowski, 1983). Phosphoramidon (1 mM), a selective inhibitor of EP 24.11 (Mumford et al., 1981), fully blocked the synthesis of Ang (1–4) and Ang (5–8) from Ang II by a vIPAG homogenate (Fig. 5B), indicating that EP 24.11

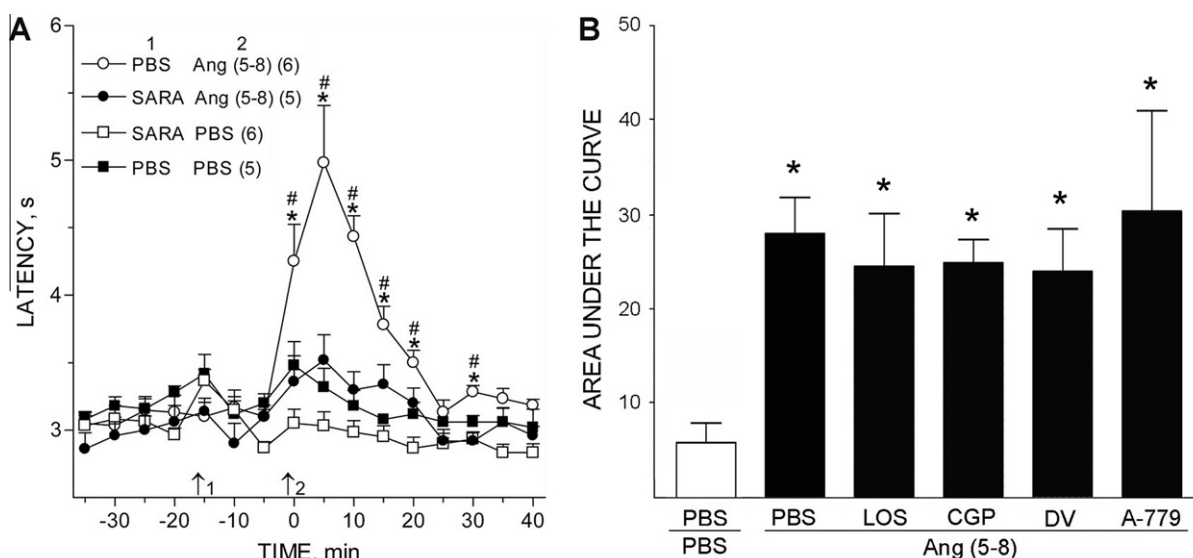


**Fig. 3.** The antinociceptive effect of Ang (5–8), detected using the tail-flick test, was Ang-R mediated, but was not blocked by specific Ang-R antagonists. (A) Ang (5–8) AA was blocked by saralasin. In the first pair of groups, phosphate-buffered saline (PBS) was injected 15 min (arrow 1) before 0.2 nmol Ang (5–8) or PBS (arrow 2), into the same PAG region. In the second pair of groups, 1.0 nmol saralasin (SARA) was injected 15 min (arrow 1) before 0.2-nmol Ang (5–8) or PBS (arrow 2), into the same PAG region. The number of rats per group (in parentheses) and their corresponding symbols are given in the upper part of the graphs. Points represent mean latency  $\pm$  S.E.M. \*Different ( $p < 0.05$ ) from PBS/PBS-treated group. #Different ( $p < 0.05$ ) from saralasin/Ang (5–8) group. (B) Ang (5–8) AA was not blocked by Losartan, CGP 42,112A, divalinal-Ang IV, and compound A-779. In the first pair of groups, phosphate-buffered saline (PBS) was injected 15 min before 0.2-nmol Ang (5–8) or PBS into the same PAG region. In five more pairs of groups, 25-pmol Losartan (LOS), 25-pmol CGP 42,112A (CGP), 0.1-nmol divalinal-Ang IV (DV) and 0.3-nmol A-779 were each injected separately 15 min before Ang (5–8) or PBS into the same vIPAG region. The areas under the time-course curves obtained from each treatment (see Suppl. Fig. S2) were calculated using the Prism (GraphPad software). The number of animals per group was 5–8. All injection volumes were 0.25  $\mu$ L. Bars represent area under the curve  $\pm$  S.E.M. \*Different ( $p < 0.05$ ) from PBS/PBS-treated group.

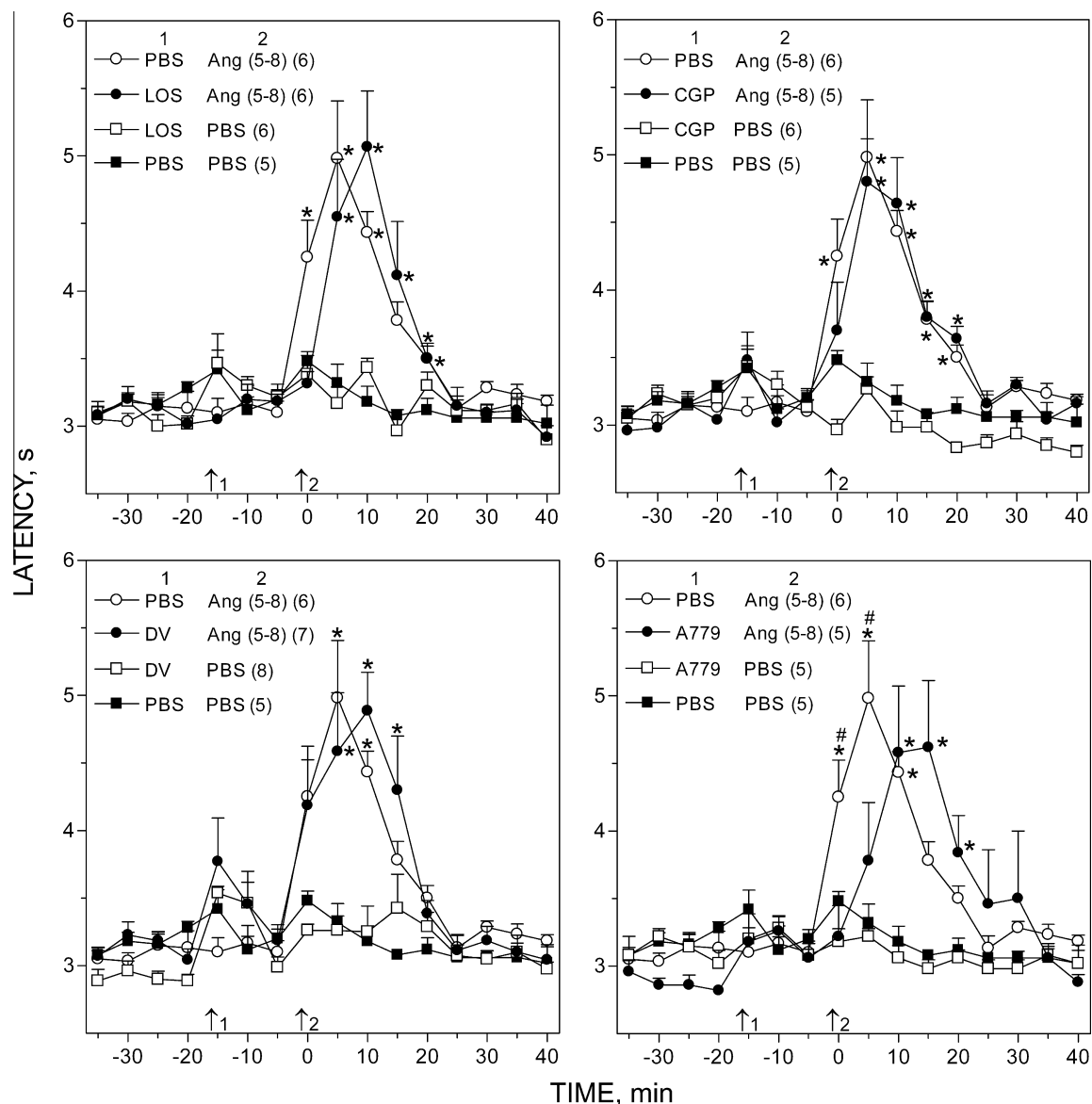


**Fig. 4.** Lack of blockade of the antinociceptive effect of Ang (5–8) by Losartan (LOS), CGP 42,112A (CGP), divalinal-Ang IV (DV) and compound A-779, detected using the tail-flick test. In the first pair of groups, PBS was injected (arrow 1) 15 min before 0.2-nmol Ang (5–8) or PBS (arrow 2) into the same vPAG region. In the second pair of groups, 25-pmol Losartan (A), 25-pmol CGP 42,112A (B), 0.1-nmol divalinal-Ang IV (C) or 0.3-nmol compound A-779 (D) was injected (arrow 1) 15 min before 0.2-nmol Ang (5–8) or PBS (arrow 2) into the same vPAG region. Points represent mean of latency  $\pm$  S.E.M.  $n = 5$ –7 for all groups. \*Different from the PBS–PBS group. #Different from group A-779/Ang (5–8).  $p < 0.05$  in all cases.

catalyzed this reaction. The initial rate of synthesis of Ang (5–8) from Ang II was 0.16 nmol/min/mg protein. Ang (1–7) was formed at about the same rate as Ang (5–8), whereas Ang III and Ang IV were formed at much lower initial rates. At 5-min incubation, Ang (5–8) accounted for 45% of recovered peptides, indicating that its formation predominated over that of other peptides. Also at 5-min incubation, the recovery of all peptide products accounted for 34% of hydrolyzed Ang II, indicating that products other than those detected were also formed. These results show that the vPAG was able to both form and inactivate Ang (5–8), as well as Ang (1–7), Ang III and Ang IV.

Ang (5–8) could also be formed from Angs other than Ang II. The incubation of Ang III with a homogenate of

vPAG-punches formed Ang (5–8) at a rate of 0.06 nmol/min/mg protein, and also formed Ang IV and Ang (4–8) at comparable rates (Fig. 5C). These results indicate that the PAG can synthesize Ang (5–8) and other short chain peptides from Ang III. The initial rate of hydrolysis of Ang (5–8) incubated alone with a vPAG homogenate was 0.55 nmol/min/mg protein. The cleavage of the Ile-His bond in Ang (5–8) can inactivate it (cf. Table 1 and results above), and could be catalyzed by an aminopeptidase. Indeed, 1.0 mM amastatin strongly inhibited the degradation of Ang (5–8) by a vPAG homogenate (Fig. 5D), indicating that Ang (5–8) can be inactivated by an amastatin-sensitive aminopeptidase. Taken together, the above results indicate that the vPAG is able to both synthesize and

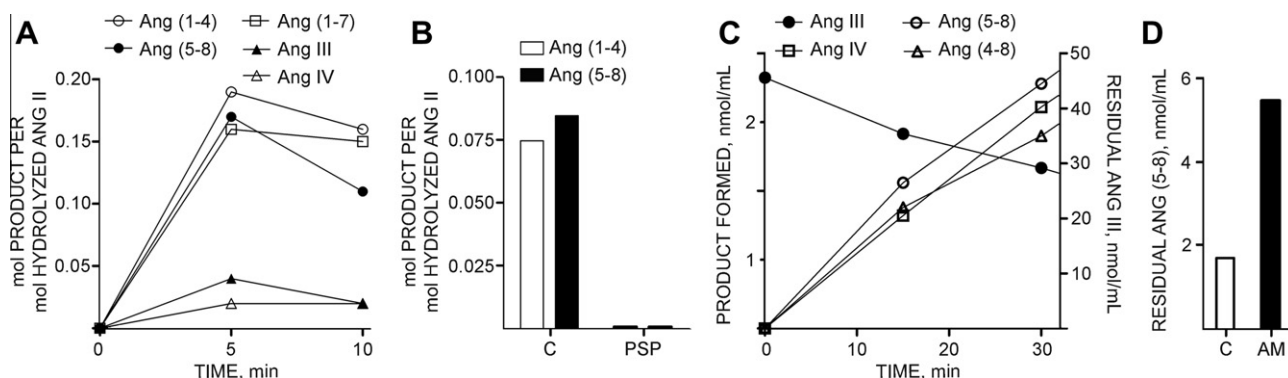


**Fig. 5.** Synthesis and inactivation of Ang (5–8) by the rat vIPAG. (A) Time-course of synthesis of Ang peptides. A homogenate of punches of vIPAG was incubated with 100  $\mu$ M Ang II in 200  $\mu$ L 50 mM Tris–HCl buffer, pH 7.5, containing 150 mM NaCl and 2.5 mg/mL homogenate protein, at 37  $^{\circ}$ C for 10 min. Product formation was expressed as the ratio mol of product/mol of hydrolyzed Ang II. The synthesis (B) and inactivation (C) of Ang (5–8) were catalyzed by EP 24.11 and an amastatin-sensitive aminopeptidase, respectively. A homogenate of punches of the vIPAG (1.27 mg/mL protein) was pre-incubated with 1 mM phosphoramidon or 1 mM amastatin in 200  $\mu$ L 50 mM Tris–HCl buffer, pH 7.5, containing 150 mM NaCl. The reaction was started by adding 50  $\mu$ M Ang II (panel C) or 10  $\mu$ M Ang (5–8) (panel D), and carried out for 30 min at 37  $^{\circ}$ C. (D) Time-course of Ang III hydrolysis and product formation. The reaction conditions were the same as in panel A, except that the substrate was 50  $\mu$ M Ang III and the protein concentration was 1.27 mg/mL. Peptides were quantified by HPLC after cleaning-up with SepPak C18. Controls were prepared the same way as incubates, except that peptidases were acid-inactivated before the addition of substrate. Materials eluting with the same retention times of peptide standards were not detected in control incubates.

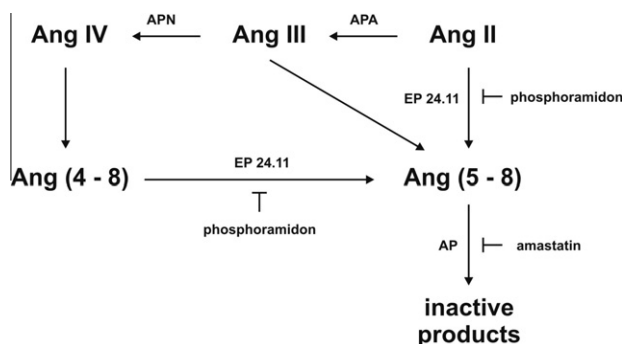


**Fig. 6.** Metabolism of Ang (5–8) by the rat vIPAG. Ang II (Asp<sup>1</sup>-Arg<sup>2</sup>-Val<sup>3</sup>-Tyr<sup>4</sup>-Ile<sup>5</sup>-His<sup>6</sup>-Pro<sup>7</sup>-Phe<sup>8</sup>); AP, aminopeptidase; APA, aminopeptidase A; APN, aminopeptidase N; EP 24.11, neprilysin; PSP, phosphoramidon; AM, amastatin. Ang (5–8) can be formed directly from Angs II and III by EP 24.11, or sequentially by cleavage of N-terminal residues starting from Ang II by aminopeptidases.

inactivate Ang (5–8) through the action of EP 24.11 and an amastatin-sensitive aminopeptidase, respectively (Fig. 6).

### Ang (5–8) elicits antinociception in the vIPAG via the NO–sGC pathway and an endogenous opioid

The NO–sGC pathway mediates several actions of Angs. Its involvement with Ang (5–8)-mediated antinociception was evaluated using the tail-flick test, and treatment with NPLA and ODQ, which are selective inhibitors of nNOS (Zhang et al., 1997) and sGC (Garthwaite, 2010), respectively. The previous injection of 0.5-nmol NPLA into the vIPAG inhibited AA of 0.2-nmol Ang (5–8) injected into the same region (Fig. 7A), suggesting that nNOS activity is required for Ang (5–8) AA. The previous injection of 1.0-nmol ODQ into the vIPAG fully blocked the antinociceptive effect of 0.2-nmol Ang (5–8) injected into the same region (Fig. 7B), suggesting that

sGC activity is required for Ang (5–8) AA. Neither 0.5-nmol NPLA nor 1.0-nmol ODQ injected alone changed the tail-flick latency. Opioid peptides can interact with Ang(s) (Rabkin, 2007). Therefore, the effect of naloxone, a non-selective opioid-R antagonist was analyzed. The previous injection of 2.5-nmol naloxone into vIPAG significantly inhibited Ang (5–8) AA (Fig. 7C), indicating that Ang (5–8) AA occurs, at least in part, via an endogenous opioid. Taken together, the above results suggest that Ang (5–8) elicited antinociception via the NO–sGC pathway and an endogenous opioid.

### Central and peripheral cardiovascular effects of Ang (5–8) are small as compared to Ang II

Angs are known for their effects on blood pressure (Bader, 2010). Therefore, we tested whether intracerebral or intravascular injection of Ang (5–8) would affect blood pressure. Doses (0.4–1.6 nmol/ $\mu$ L) of Ang (5–8) that were within the dose range used for the antinociception dose–response curve were injected into the vIPAG, to permit a comparison between the effects of Ang (5–8) on antinociception and blood pressure changes, using Ang II (0.1–1.6 nmol/ $\mu$ L) as a control. Injecting different doses of Ang (5–8) (0.4–1.6 nmol/0.2  $\mu$ L) into the vIPAG (Fig. 8A) of unanesthetized Wistar rats caused dose-related pressor and bradycardic responses, with an estimated ED<sub>50</sub> for the pressor response of 0.75 nmol (Fig. 8B). The maximal pressor response to the injection of Ang (5–8) into the vIPAG was 2.7-fold smaller ( $\Delta$ MAP = +16  $\pm$  3 mmHg) than that evoked by the same dose of Ang II ( $\Delta$ MAP = +44  $\pm$  6 mmHg). The maximal increase of HR elicited by Ang (5–8) was approximately threefold smaller ( $\Delta$ HR = –21  $\pm$  3 bpm) than that elicited by Ang II ( $\Delta$ HR = –61  $\pm$  7 bpm) injected into the same region (Fig. 8C).

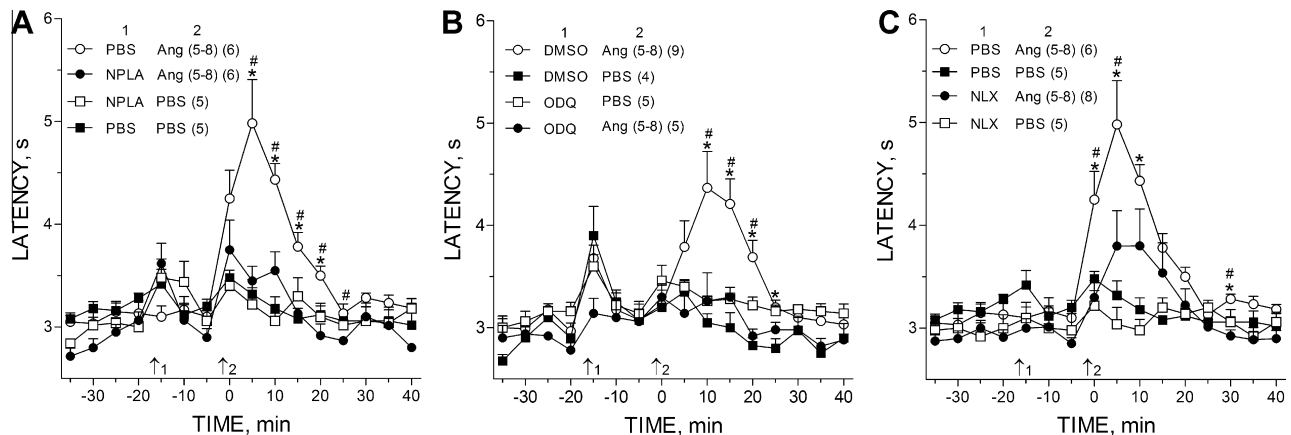


**Fig. 7.** The antinociceptive effect of Ang (5–8) in the vPAG, detected using the tail-flick test, is NO, sGC and opioid-dependent. (A) The antinociceptive effect of Ang (5–8) injection into the vPAG was blocked by the inhibition of neuronal NO synthase. In the first pair of groups, PBS was injected 15 min (arrow 1) before 0.2-nmol Ang (5–8) or PBS (arrow 2), into the same PAG region. In the second pair of groups, 0.5-nmol N<sup>ω</sup>-propyl-L-arginine (NPLA) was injected 15 min (arrow 1) before 0.2-nmol Ang (5–8) or PBS (arrow 2). \*Different ( $p < 0.05$ ) from PBS/PBS group. #Different ( $p < 0.05$ ) from NPLA/Ang (5–8)-treated group. (B) The antinociceptive effect of Ang (5–8) injection into vPAG was blocked by the inhibition of soluble guanylyl cyclase. In the first pair of groups, PBS containing 10% (v/v) dimethylsulfoxide (DMSO) was injected 15 min (arrow 1) before 0.2-nmol Ang (5–8) or PBS (arrow 2). \*Different ( $p < 0.05$ ) from DMSO/PBS group. #Different ( $p < 0.05$ ) from ODQ/Ang (5–8)-treated group. (C) The antinociceptive effect of Ang (5–8) was blocked by an opioid-R antagonist. In the first pair of groups, PBS was injected 15 min (arrow 1) before 0.2-nmol Ang (5–8) or PBS (arrow 2). In the second pair of groups, 2.5-nmol naloxone was injected 15 min (arrow 1) before 0.2-nmol Ang (5–8) or PBS (arrow 2). \*Different ( $p < 0.05$ ) from PBS/PBS group. #Different ( $p < 0.05$ ) from naloxone/Ang (5–8) group. The number of rats per group (in parentheses) and their corresponding symbols are given in the upper part of the graphs. All injection volumes were 0.25  $\mu$ L. Points represent mean latency  $\pm$  S.E.M.

Doses of Ang (5–8) that were 7.5-fold or 20-fold higher than those that elicited a maximal antinociceptive response were used for i.c.v. or intravascular injections, respectively, because in pilot studies the injection of doses (0.4–0.8 nmol) that elicited maximal antinociceptive response led to undetectable changes of blood pressure (data not shown). The i.c.v. administration of 8-nmol Ang (5–8) in unanesthetized Wistar rats evoked a 10-mmHg increase in the MAP (Fig. 8D). This increase was 2.5-fold smaller than that elicited by an i.c.v. injection of 60-pmol Ang II, a dose of Ang II two orders of magnitude smaller than that of Ang (5–8), indicating that Ang (5–8) did not elicit appreciable pressor responses at periventricular sites responsive to Ang II. HR did not decrease with 8-nmol Ang (5–8), but decreased 27 bpm following the injection of 60-pmol Ang II (Fig. 8E). Intra-arterial or intra-venous injection of 3-nmol Ang (5–8) in normal, awaken Wistar rats elicited pressor responses that were fivefold or 3.7-fold smaller than those elicited by a 10-fold smaller dose of Ang II, respectively (Fig. 8F), without appreciably affecting HR (Fig. 8G). The results above suggest that Ang (5–8) exhibits a very small effect on blood pressure.

#### Effect of Ang (5–8) on isolated smooth muscles

Ang (5–8) relaxed pre-contracted aorta ( $pD_2 = 6.56 \pm 0.2$ ,  $n = 10$ ) to 33% of the initial force ( $33.3 \pm 7.3\%$ ,  $n = 10$ ), and did not alter rat aorta baseline force (Fig. 9A). Sodium nitroprusside was used as a control, and fully relaxed the pre-contracted aorta with a potency ( $pD_2 = 7.54 \pm 0.07$ ,  $n = 9$ ) 10 times higher than that of Ang (5–8) ( $EC_{50} = 0.28 \mu$ M;  $p < 0.001$ ) (Fig. 9B). The vasorelaxation effect of Ang

(5–8) was fully prevented by pre-treating the aorta with 100  $\mu$ M N<sup>G</sup>-nitro-L-arginine ( $p < 0.001$ ), a constitutive NO synthase inhibitor (Fig. 9A). These results indicate that Ang (5–8) can relax the rat aorta via NO production by the endothelium. Ang (5–8) elicited a barely detectable contraction of the isolated guinea-pig ileum in the dose range  $10^{-8}$ – $10^{-6}$  M, in contrast to Ang II (Fig. 9C). The above results indicate that Ang (5–8) exhibited weak or no activity on several models of *in vitro* smooth muscle. Taken together, the results on blood pressure and smooth muscle preparations suggest that the effect of Ang (5–8) can be selective for antinociception.

## DISCUSSION

The present work provides the first evidences for the following: (i) the tetrapeptide Ang (5–8) was the smallest Ang-peptide that elicited an antinociceptive effect upon injection into the vPAG; (ii) Ang (5–8) elicited region-specific, dose-dependent and Ang-R-mediated antinociception in the vPAG that does not appear to be mediated by any known Ang-Rs; (iii) the vPAG can synthesize Ang (5–8) from Ang II through cleavage of the Tyr-Ile peptide bond by EP 24.11; other sources of Ang (5–8) formation include Ang III and Ang (4–8); (iv) the inactivation of Ang (5–8) can be carried out by an amastatin-sensitive aminopeptidase; (v) the AA of Ang (5–8) occurred via the NO–sGC pathway and an endogenous opioid in the vPAG; and (vi) the effect of Ang (5–8) on vascular and intestinal smooth muscles was small or absent.

The PAG is a key relay station in the processing of nociceptive and antinociceptive information in the CNS

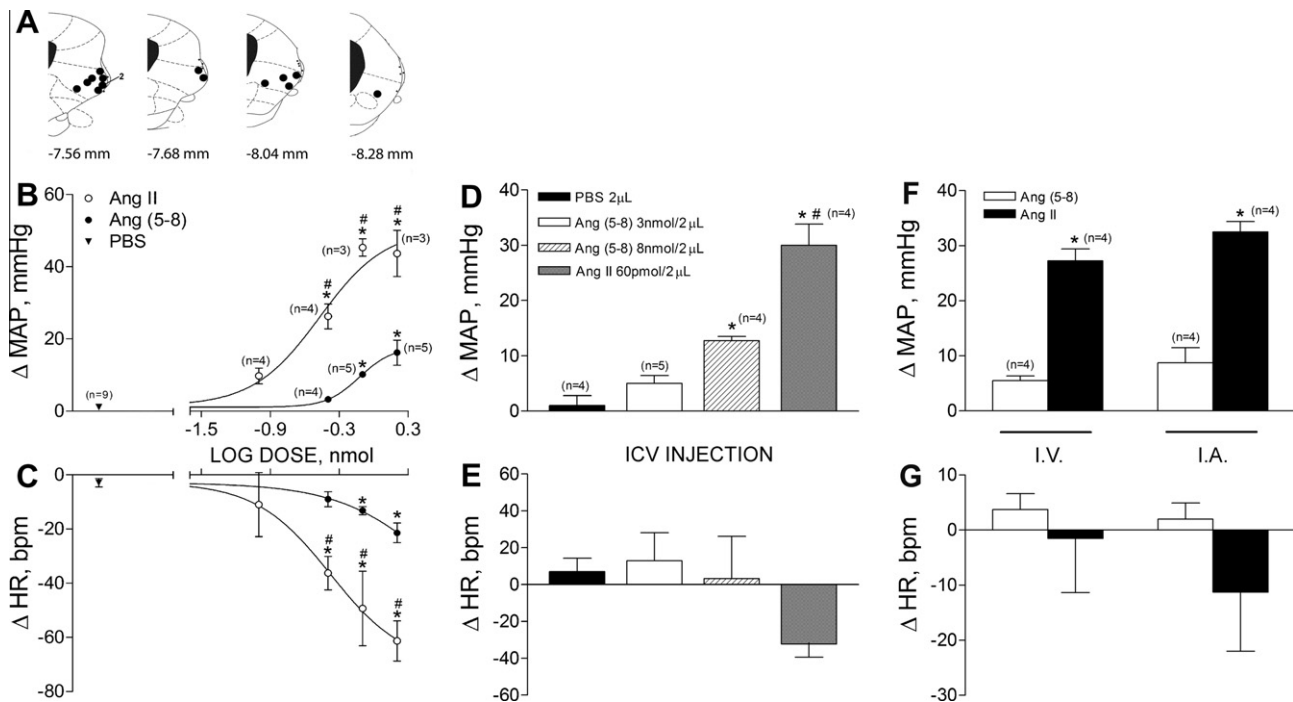


**Fig. 8.** The administration of Ang (5–8) into different body compartments elicits small or no changes of cardiovascular parameters compared to angiotensin II. (A–C) Administration into vIPAG. (A) Coronal sections showing the location of Ang (5–8) (filled circles) and Ang II (open circles) injection sites into the vIPAG that have led to changes in mean arterial pressure ( $\Delta$ MAP) and heart rate ( $\Delta$ HR). Numbers indicate the distance from bregma. (B, C) Mean arterial pressure (panel B;  $\Delta$ MAP, mmHg) and heart rate (panel C;  $\Delta$ HR, bpm) changes evoked by Ang II (0.1, 0.4, 0.8, 1.6 nmol/0.20  $\mu$ L; open circles), Ang (5–8) (0.4, 0.8, 1.6 nmol/0.20  $\mu$ L; filled circles) or PBS (0.20  $\mu$ L; filled triangles) microinjected into the vIPAG ( $n = 15$ ). Baseline MAP and HR for Ang II were  $91 \pm 2.4$  mmHg and  $350 \pm 11$  bpm ( $n = 11$ ), and  $94 \pm 3$  mmHg and  $362 \pm 14$  bpm for Ang (5–8), respectively. Nonlinear regression analyses indicated a significant correlation between dose and pressor ( $r^2 = 0.92$ ,  $df = 19$ ,  $p < 0.05$ ) or bradycardiac ( $r^2 = 0.75$ ,  $df = 19$ ,  $p < 0.05$ ) responses for Ang II, as well as for Ang (5–8) (dose and pressor ( $r^2 = 0.76$ ,  $df = 19$ ,  $p < 0.05$ ) or bradycardiac ( $r^2 = 0.67$ ,  $df = 19$ ,  $p < 0.05$ )). \*Significantly different from control (AngII:  $\Delta$ MAP,  $F_{(4,18)} = 67.6$ ,  $p < 0.0001$ ;  $\Delta$ HR,  $F_{(4,18)} = 13.6$ ,  $p < 0.0001$ ; Ang (5–8):  $\Delta$ MAP,  $F_{(3,19)} = 20.4$ ,  $p < 0.0001$ ;  $\Delta$ HR,  $F_{(3,19)} = 12.7$ ,  $p < 0.0001$ ; one-way ANOVA, Bonferroni's post hoc test). #Statistically different AngII vs Ang (5–8) compared to the same dose ( $\Delta$ MAP,  $F_{(6,21)} = 28$ ,  $p < 0.0001$ ;  $\Delta$ HR,  $F_{(6,21)} = 7.7$ ,  $p < 0.0002$ ; one-way ANOVA, Bonferroni's post hoc test). Data are expressed as the means  $\pm$  S.E.M. (D, E) Administration into the lateral ventricle. Changes of mean arterial pressure ( $\Delta$ MAP, mmHg) (D) and heart rate ( $\Delta$ HR, bpm) (E) were evoked by 3 and 8 nmol/2  $\mu$ L Ang (5–8), 60 pmol/2  $\mu$ L Ang II or 2  $\mu$ L PBS injected into the lateral ventricle of unanesthetized rats. \*Different from control ( $\Delta$ MAP,  $F_{(2,10)} = 16.9$ ,  $p = 0.0006$ ;  $\Delta$ HR,  $F_{(2,10)} = 0.32$ ,  $p = 0.73$ ; one-way ANOVA, Bonferroni's post hoc test). #Different from both doses of Ang (5–8) ( $\Delta$ MAP,  $F_{(3,13)} = 33.9$ ,  $p < 0.0001$ ;  $\Delta$ HR,  $F_{(3,13)} = 1.83$ ,  $p = 0.19$ , one-way ANOVA, Bonferroni's post hoc test). Data are expressed as the means  $\pm$  S.E.M. (F, G) Intravascular administration. Ang (5–8) (3 nmol/kg body weight; open columns) or Ang II (0.3 nmol/kg body weight; filled columns) were injected into the femoral vein (i.v.) or into the carotid artery (i.a.) of anesthetized rats and  $\Delta$ MAP (mmHg) (F) or  $\Delta$ HR (bpm) (G) were recorded. \*Statistically significant compared to drug by the route administered (i.v.:  $\Delta$ MAP,  $t = 9.3$ ,  $df = 6$ ,  $p = 0.0001$ ;  $\Delta$ HR,  $t = 0.5$ ,  $p = 0.62$ ; i.a.:  $\Delta$ MAP,  $t = 7.1$ ,  $df = 6$ ,  $p = 0.0004$ ;  $\Delta$ HR,  $t = 1.2$ ,  $p = 0.28$ , unpaired Student's  $t$ -test). Data are expressed as the means  $\pm$  S.E.M.

(Millan, 2002). Electrical stimulation of the vIPAG subdivision depresses the responses of spinal cord neurons to peripheral noxious stimulation (Sandkuhler et al., 1996), whereas persistent noxious stimulation increases PAG activity (Monhemius et al., 2001). The tail-flick and incision allodynia models involve a tail flick and a paw withdrawal upon noxious or allodynic stimulation of the tail or the incised paw, respectively, and both depend on a spinal reflex. The tail-flick test involves a brief (up to 6 s) noxious stimulus. In contrast, incision allodynia involves longer lasting (tested up to 50 min in this study) noxious inputs provided by a surgical incision. In incision allodynia, the noxious input is sufficient to permit detection of the activation of supraspinal structures that control spinal nociceptive inputs (Villarreal et al., 2004; Pelegrini-da-Silva et al., 2005, 2009), whereas in the tail-flick test this activation has not been detected (the present study; Azami et al., 2001). The antinociceptive effect of Ang (5–8) on both

pain models indicates that it inhibits and/or activates facilitatory or inhibitory descending nociceptive pathways to the spinal cord, respectively. The dose of Ang (5–8) that elicited maximal antinociception was 74-fold lower than that of morphine injected into the vIPAG, which is a region very sensitive to morphine (Jensen and Yaksh, 1989). The dose–response curve for Ang (5–8) was bell-shaped. Bell-shaped dose–response curves have frequently been interpreted as due to a dual effect of an agonist, as exemplified for substance P (Frederickson et al., 1978). The mechanism generating the bell-shaped dose–response curve for Ang (5–8) has not been elucidated. Thus, Ang (5–8) injected into the vIPAG elicits a strong, dose-dependent and region-specific modulation of antinociception.

The involvement of Ang-Rs on pain modulation elicited by Ang (5–8) was studied using saralasin ([Sar<sup>1</sup>-Ala<sup>8</sup>]-Ang II), a non-selective Ang-R antagonist that can display partial agonist activity at high doses (De

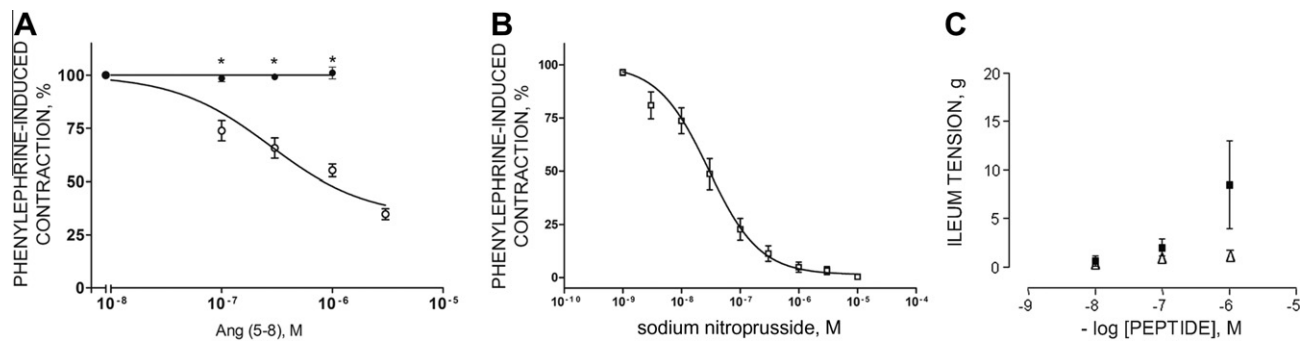


**Fig. 9.** Effect of Ang (5–8) on isolated preparations of vascular and intestinal smooth muscles. (A) Ang (5–8) was added cumulatively in the presence (open circles,  $n = 10$ ) or absence of functional endothelium ( $100 \mu\text{M}$   $\text{N}^G$ -nitro-L-arginine, closed circles,  $n = 8$ ). (B) concentration–response curve to sodium nitroprusside ( $n = 9$ ). Data are expressed as the means  $\pm$  S.E.M. of individual experiments performed with different animals. Aorta relaxation data were plotted as the means  $\pm$  S.E.M. Data from isometric contraction assays were compared by unpaired Student's  $t$ -test. \*Different from Ang (5–8) in the presence of functional endothelium ( $p < 0.001$ ). (C) dose–response curve for the contractile effect of different concentrations of Ang II (closed squares) or Ang (5–8) (open triangles) on the isolated guinea-pig ileum preparation. Data represent the means  $\pm$  S.E.M. of at least four preparations.

Gasparo et al., 2000), and Losartan, CGP 42,112A, divalinal-Ang IV and compound A-779, which are specific and selective antagonists of Ang-R types 1, 2, 4 (De Gasparo et al., 2000), and the Mas receptor (Santos et al., 2003), respectively. Losartan and CGP 42,112A were used here at doses 10–100-fold higher than those that fully blocked receptor-mediated AA of Angs II and III in the vPAG (Pelegri-da-Silva et al., 2005, 2009). The doses of divalinal-Ang IV and A-779 used here were comparable to or higher than those used by Wright and Harding (1995) and Santos et al. (2003), respectively. The inhibition of Ang (5–8) AA by saralasin, but not by the specific antagonists used here, suggests that Ang (5–8) might act through an unidentified receptor in the PAG.

The formation of equimolar amounts of Ang (1–4) and Ang (5–8) from Ang II (Asp<sup>1</sup>-Arg<sup>2</sup>-Val<sup>3</sup>-Tyr<sup>4</sup>-Ile<sup>5</sup>-His<sup>6</sup>-Pro<sup>7</sup>-Phe<sup>8</sup>) by vPAG punches (this work) indicates that the cleavage of the Tyr<sup>4</sup>-Ile<sup>5</sup> peptide bond was catalyzed by an endopeptidase. Endopeptidases that cleave Tyr-Ile bond include: EP 24.11 (EC 3.4.24.11, neprilysin) (Almenoff and Orłowski, 1983), EP 24.15 (EC 3.4.24.15, thimet oligopeptidase) (Rioli et al., 1998), EP 24.16 (EC 3.4.24.16, neurolysin) (Rioli et al., 1998), and NUDEL-oligopeptidase (EC 3.4.22.19; Oliveira et al., 1976; Medeiros et al., 1992). Tyr<sup>4</sup>-Ile<sup>5</sup> bond cleavage by PAG was fully inhibited by phosphoramidon (this work), a compound that specifically inhibits EP 24.11 (Mumford et al., 1981), but not brain endopeptidases EP 24.15, EP 24.16 (Dahms and Mentlein, 1992) and NUDEL-oligopeptidase (Hayashi et al., 2005). Thus, Ang (5–8) formation from Ang II by the vPAG can be catalyzed by EP 24.11.

Ang (5–8) was also formed from Ang III by PAG at a rate 17-fold lower than that from Ang II, indicating that, *in vitro*, the cleavage of the Tyr-Ile bond of Ang II predominates over that of Ang III. The cleavage of the Tyr-Ile bond in Ang III can also be carried out by EP 24.11 (Karamyan and Speth, 2007). A third pathway for Ang (5–8) synthesis shown here involves the sequential cleavage of Ang II by aminopeptidases (see Fig. 6), which is similar to aminopeptidase pathways in primary

cultures of neuronal and glial cells (Hermann et al., 1989) as well as vascular smooth muscle cells (Mentlein and Roos, 1996). Therefore, it appears that the vPAG can form Ang (5–8) by several enzymatic pathways, from several substrates, and at widely differing rates. Ang (5–8) degradation can be carried out by several peptidases, among them an amastatin-sensitive aminopeptidase (this work), aminopeptidase N (Mentlein and Roos, 1996), carboxypeptidase P (EC 3.4.17.16; Hedeager-Sorensen and Kenny, 1985), and prolyl-endopeptidase (Wilk, 1983), leading to tri- and dipeptides, and free amino acids. Because di- and tripeptides formed from Ang (5–8) did not exhibit AA (the present work), the cleavage of any peptide bond in Ang (5–8) can inactivate it. The concerted action of PAG peptidases to modulate Ang-peptide levels at the vicinity of an Ang-R is a complex process. The assignment of the relative contribution of each metabolic pathway to Ang (5–8) metabolism in the PAG remains to be established.

Several Ang-peptides exhibited AA upon injection into different brain regions. In the vPAG, Ang III AA appears to predominate over Ang II AA (Pelegri-da-Silva et al., 2005, 2009). Ang IV and Ang (1–7) now include antinociception in their activity spectra. Ang (5–8) was considered inactive or requiring 100-fold higher doses than Ang II to exhibit activity on classic Ang II actions, such as pressor (Khosla et al., 1974), dipsogenic (Tonnaer et al., 1982) or spasmogenic (Khosla et al., 1974) activities. Indeed, the injection of Ang (5–8) into the vPAG, brain ventricle or vasculature of rats leads to smaller or undetectable effects compared to Ang II, to a weak relaxation of isolated aorta and to no effect on isolated guinea-pig ileum (the present work). Therefore, the present findings suggest that Ang (5–8) is more selective to elicit antinociception than blood pressure changes. This property of Ang (5–8) can be advantageous for its use as a leading compound for the synthesis of new compounds to be used as new analgesic drugs and/or as tools to study the RAS.

Ang (5–8) was considered an inactive degradation product of Ang II (Mentlein and Roos, 1996). A recent

report on Ang (5–8) activity describes its ability to inhibit cell viability and BrdU incorporation in lactosomatotroph (GH3) cells in culture, which was not blocked by AT<sub>1</sub>R, AT<sub>2</sub>R or AT<sub>4</sub>R (Ptasinska-Wnuk et al., 2012). Ang-peptides derived from Ang (5–8) have not exhibited AA upon injection into the vPAG (this work). Thus, Ang (5–8) contains the smallest amino acid sequence that is necessary and sufficient to elicit a strong antinociceptive effect upon injection into the vPAG. Ang (4–8) also exhibits AA, and its effect may be due, at least in part, to its conversion to Ang (5–8). Therefore, Ang II, Ang III and Ang (5–8), and most likely Angs IV, (4–8) and (1–7), participate in the modulation of nociception by the rat PAG. The multiplicity of Ang peptides and Ang-metabolizing peptidases found to be active in the PAG resembles that found in the periphery and nervous system, where regulatory and counter-regulatory mechanisms can be exerted by the concerted action of several Angs, Ang-Rs and peptidases (von Bohlen und Halbach and Albrecht, 2006; Bader, 2010). Additional layers of nociception regulation are represented by other pathways relaying in the PAG that can modulate noxious information through known pain mediators, such as serotonin, Leu- and Met-enkephalin,  $\beta$ -endorphin, glutamate and GABA (Basbaum and Fields, 1984; Millan, 2002).

The neurotransmitter/neuromodulator NO has been shown to contribute to pain mechanisms. However, there are conflicting reports regarding NO involvement on nociception processing. NO donors have a dual effect on nociception, acting either as antinociceptive or pronociceptive, depending on the dose, region, pain model and type of donor used (Sousa and Prado, 2001; Schmidtko et al., 2009). However, experiments using selective NOS inhibitors and mice deficient in NOS isoforms indicated the involvement of endogenous nNOS in the spinal cord during the development and maintenance of inflammatory and neuropathic pain (Schmidtko et al., 2009). In the tail-flick model, the inhibition of nNOS by NPLA blocked Ang (5–8) AA (the present report), suggesting that Ang (5–8) acts via NO. The localization of nNOS (Onstott et al., 1993) in the PAG provides a cellular basis for a NO-ergic mechanism of Ang (5–8) AA. In addition, N<sup>G</sup>-nitro-L-arginine, a non-selective NOS inhibitor, blocked the Ang (5–8)-induced aorta relaxation, indicating NO is also involved in the weak vascular relaxing effect of Ang (5–8). Most of NO physiological effects can be ascribed to cGMP produced by sGC that has been activated by NO (Murad, 1994; Garthwaite, 2010). This mechanism could also be operating in the PAG because the administration of the phosphodiesterase-5 inhibitor sildenafil reduced inflammatory pain (Araiza-Saldana et al., 2010) and because the injection of ODQ into vPAG blocked Ang (5–8)-elicited antinociception (the present report). The above results and discussion suggest that Ang (5–8) can elicit antinociception via NO/sGC.

sGC can generate cGMP (Murad, 1994; Garthwaite, 2010). Cyclic-GMP targets cGMP-dependent protein kinase, cyclic nucleotide-hydrolyzing phosphodiesterases

and cyclic nucleotide gated cation channels, thus providing mechanisms to the modulation of transmitter release, particularly glutamate (Feil and Kleppisch, 2008). Glutamate and glutamate receptors occur in neurons in PAG (Beitz, 1995), and glutamate injected into the PAG elicits antinociception (Jensen and Yaksh, 1992). Glutamate acting via NMDA receptors and NO production can also modulate the transmission of opioid pain-inhibitory signals (Javanmardi et al. 2005). Analgesia evoked from the PAG ventrolateral column is opioid-dependent (Beitz, 1995). The inhibition of opioid-R in the PAG by the non-selective antagonist naloxone led to the blockade of Ang (5–8) AA, suggesting that Ang (5–8) acts through an opioid-based mechanism. However, it is not presently known whether Ang (5–8) antinociception occurs by two separate mechanisms, e.g., an opioid-based and a NO/sGC/cGMP-based mechanism, or whether these two mechanisms are linked. Taken together, the present results and discussion suggest that Ang (5–8) can modulate antinociception in the vPAG by direct or indirect mechanisms, acting on NO/sGC pathway and an endogenous opioid.

## CONCLUSION

We provide here the first evidence that Ang (5–8) modulates antinociception in the vPAG via an unknown Ang-R. The effect of Ang (5–8) seems to be selective for antinociception, on the basis of its lack of activity on both central and peripheral models of blood pressure analysis, and on isolated smooth muscle preparations. The vPAG synthesizes Ang (5–8) from Ang II, Ang III, and Ang IV, and inactivates Ang (5–8) efficiently by aminopeptidases. The antinociceptive activity of Ang (5–8) occurs via the NO–sGC pathway and an endogenous opioid in vPAG.

## AUTHOR CONTRIBUTIONS

A.P.S., A.R.M., C.L.M.S., G.G.P., K.G.B., L.M.G. and M.A.J. performed research; A.R.M., C.L.M.S., F.M., F.M.A.C., M.A.J. and W.A.P. designed experiments; A.R.M., C.L.M.S., F.M., F.M.A.C. and W.A.P. wrote the paper.

*Acknowledgments*—This work was supported by CNPq (grants 306008/2009-2 and 561151/2010-5 to A.R.M., 472474/2010-3 and 476394/2012-0 to C.L.M.S., 159841/2010-0 to K.G.B.), CAPES (to A.R.M.) and FAPESP (2008/06676-8 to J.B.P.).

## REFERENCES

- Almenoff J, Orlowski M (1983) Membrane-bound kidney neutral metalloendopeptidase: interaction with synthetic substrates, natural peptides, and inhibitors. *Biochemistry* 22:590–599.
- Antunes-Rodrigues J, de Castro M, Elias LL, Valenca MM, McCann SM (2004) Neuroendocrine control of body fluid metabolism. *Physiol Rev* 84:169–208.
- Araiza-Saldana CI, Rocha-Gonzalez HI, Ambriz-Tututi M, Castaneda-Corral G, Caram-Salas NL, Hong E, Granados-Soto V (2010) Sildenafil and glyceryl trinitrate reduce tactile allodynia in streptozotocin-injected rats. *Eur J Pharmacol* 631:17–23.

- Azami J, Llewelyn MB, Roberts MH (1980) An extra-fine assembly for intracerebral injection. *J Physiol* 303:18P–19P.
- Azami J, Green DL, Roberts MH, Monhemius R (2001) The behavioral importance of dynamically activated descending inhibition from the nucleus reticularis gigantocellularis pars alpha. *Pain* 92:53–62.
- Bader M (2010) Tissue renin–angiotensin–aldosterone systems: targets for pharmacological therapy. *Annu Rev Pharmacol Toxicol* 50:439–465.
- Baltatu OC, Campos LA, Bader M (2011) Local renin–angiotensin system and the brain: a continuous quest for knowledge. *Peptides* 32:1083–1086.
- Basbaum AI, Fields HL (1984) Endogenous pain control systems: brainstem spinal pathways and endorphin circuitry. *Annu Rev Neurosci* 7:309–338.
- Beitz A (1995) Periaqueductal gray. In: Paxinos G, editor. *The rat nervous system*. New York: Academic Press. p. 173–182.
- Brennan TJ, Vandermeulen EP, Gebhart GF (1996) Characterization of a rat model of incisional pain. *Pain* 64:493–501.
- Dahms P, Mentlein R (1992) Purification of the main somatostatin-degrading proteases from rat and pig brains, their action on other neuropeptides, and their identification as endopeptidases 24.15 and 24.16. *Eur J Biochem* 208:145–154.
- De Gasparo M, Catt KJ, Inagami T, Wright JW, Unger T (2000) International Union of Pharmacology. XXIII. The angiotensin II receptors. *Pharmacol Rev* 52:415–472.
- Feil R, Kleppisch T (2008) NO/cGMP-dependent modulation of synaptic transmission. In: Südhof TC, Starke K, editors. *Pharmacology of neurotransmitter release*. Berlin: Springer-Verlag. p. 529–560.
- Frederickson RC, Burgis V, Harrell CE, Edwards JD (1978) Dual actions of substance P on nociception: possible role of endogenous opioids. *Science* 199:1359–1362.
- Garthwaite J (2010) New insight into the functioning of nitric oxide-receptive guanylyl cyclase: physiological and pharmacological implications. *Mol Cell Biochem* 334:221–232.
- Georgieva D, Georgiev V (1999) The role of angiotensin II and of its receptor subtypes in the acetic acid-induced abdominal constriction test. *Pharmacol Biochem Behav* 62:229–232.
- Haulica I, Neamtu C, Stratone A, Petrescu Gh, Branisteanu D, Rosca V, Slatineanu S (1986) Evidence for the involvement of cerebral renin–angiotensin system (RAS) in stress analgesia. *Pain* 27:237–245.
- Hayashi MA, Portaro FC, Bastos MF, Guerreiro JR, Oliveira V, Gorrao SS, Tambourgi DV, Sant'anna OA, Whiting PJ, Camargo LM, Konno K, Brandon NJ, Camargo AC (2005) Inhibition of NUDEL (nuclear-distribution element-like)-oligopeptidase activity by disrupted-in-schizophrenia 1. *Proc Natl Acad Sci U S A* 102:3828–3833.
- Hedeager-Sorensen S, Kenny AJ (1985) Proteins of the kidney microvillar membrane. Purification and properties of carboxypeptidase P from pig kidneys. *Biochem J* 229:251–257.
- Hermann K, Phillips MI, Raizada MK (1989) Metabolism of angiotensin peptides by neuronal and glial cultures from rat brain. *J Neurochem* 52:863–868.
- Javanmardi K, Parviz M, Sadr SS, Keshavarz M, Minaii B, Dehpour AR (2005) Involvement of N-methyl-D-aspartate receptors and nitric oxide in the rostral ventromedial medulla in modulating morphine pain-inhibitory signals from the periaqueductal grey matter in rats. *Clin Exp Pharmacol Physiol* 32:585–589.
- Jensen TS, Yaksh TL (1989) Comparison of the antinociceptive effect of morphine and glutamate at coincidental sites in the periaqueductal gray and medial medulla in rats. *Brain Res* 476:1–9.
- Jensen TS, Yaksh TL (1992) The antinociceptive activity of excitatory amino acids in the rat brainstem: an anatomical and pharmacological analysis. *Brain Res* 569:255–267.
- Karamyan VT, Speth RC (2007) Enzymatic pathways of the brain renin–angiotensin system: unsolved problems and continuing challenges. *Regul Pept* 143:15–27.
- Khosla MC, Smeby RR, Bumpus FM (1974) Structure–activity relationship in angiotensin II analogs. In: Page IH, Bumpus FM, editors. *Angiotensin*. Heidelberg: Springer-Verlag. p. 126–161.
- Lowry OH, Rosebrough NJ, Farr AL, Randall RJ (1951) Protein measurement with the Folin phenol reagent. *J Biol Chem* 193:265–275.
- Marques-Lopes J, Pinto M, Pinho D, Morato M, Patinha D, Albino-Teixeira A, Tavares I (2009) Microinjection of angiotensin II in the caudal ventrolateral medulla induces hyperalgesia. *Neuroscience* 158:1301–1310.
- Medeiros MS, Iazigi N, Camargo AC, Oliveira EB (1992) Distribution and properties of endo-oligopeptidases A and B in the human neuroendocrine system. *J Endocrinol* 135:579–588.
- Mentlein R, Roos T (1996) Proteases involved in the metabolism of angiotensin II, bradykinin, calcitonin gene-related peptide (CGRP), and neuropeptide Y by vascular smooth muscle cells. *Peptides* 17:709–720.
- Millan MJ (2002) Descending control of pain. *Prog Neurobiol* 66:355–474.
- Monhemius R, Green DL, Roberts MH, Azami J (2001) Periaqueductal grey mediated inhibition of responses to noxious stimulation is dynamically activated in a rat model of neuropathic pain. *Neurosci Lett* 298:70–74.
- Mumford RA, Pierzchala PA, Strauss AW, Zimmerman M (1981) Purification of a membrane-bound metalloendopeptidase from porcine kidney that degrades peptide hormones. *Proc Natl Acad Sci U S A* 78:6623–6627.
- Murad F (1994) The nitric oxide–cyclic GMP signal transduction system for intracellular and intercellular communication. *Recent Prog Horm Res* 49:239–248.
- Oliveira EB, Martins AR, Camargo AC (1976) Isolation of brain endopeptidases: influence of size and sequence of substrates structurally related to bradykinin. *Biochemistry* 15:1967–1974.
- Onstott D, Mayer B, Beitz AJ (1993) Nitric oxide synthase immunoreactive neurons anatomically define a longitudinal dorsolateral column within the midbrain periaqueductal gray of the rat: analysis using laser confocal microscopy. *Brain Res* 610:317–324.
- Palkovits M, Brownstein MJ (1983) Microdissection of brain areas by the punch technique. In: Cuello AC, editor. *Brain Microdissection Techniques*. New York: John Wiley & Sons. p. 1–36.
- Paxinos G, Watson C (1986) *The rat brain in stereotaxic coordinates*. New York: Academic Press.
- Pelegri-da-Silva A, Prado WA, Juliano MA, Wilk S, Martins AR (2002) High-performance liquid chromatographic separation of renin–angiotensin system peptides and most of their metabolic fragments. *J Chromatogr B: Anal Technol Biomed Life Sci* 780:301–307.
- Pelegri-da-Silva A, Martins AR, Prado WA (2005) A new role for the renin–angiotensin system in the rat periaqueductal gray matter: angiotensin receptor-mediated modulation of nociception. *Neuroscience* 132:453–463.
- Pelegri-da-Silva A, Rosa E, Guethe LM, Juliano MA, Prado WA, Martins AR (2009) Angiotensin III modulates the nociceptive control mediated by the periaqueductal gray matter. *Neuroscience* 164:1263–1273.
- Prado WA, Pelegri-da-Silva A, Martins AR (2003) Microinjection of renin–angiotensin system peptides in discrete sites within the rat periaqueductal gray matter elicits antinociception. *Brain Res* 972:207–215.
- Ptasinska-Wnuk D, Mucha SA, Lawnicka H, Fryczak J, Kunert-Radek J, Pawlikowski M, Stepień H (2012) The effects of angiotensin peptides and angiotensin receptor antagonists on the cell growth and angiogenic activity of GH3 lactosomatotroph cells in vitro. *Endocrine* 42:88–96.
- Rabkin SW (2007) Endogenous kappa opioids mediate the action of brain angiotensin II to increase blood pressure. *Neuropeptides* 41:411–419.
- Rioli V, Kato A, Portaro FC, Cury GK, te Kaat K, Vincent B, Checler F, Camargo AC, Glucksman MJ, Roberts JL, Hirose S, Ferro ES

- (1998) Neuropeptide specificity and inhibition of recombinant isoforms of the endopeptidase 3.4.24.16 family: comparison with the related recombinant endopeptidase 3.4.24.15. *Biochem Biophys Res Commun* 250:5–11.
- Sandkuhler J, Treier AC, Liu XG, Ohnimus M (1996) The massive expression of c-fos protein in spinal dorsal horn neurons is not followed by long-term changes in spinal nociception. *Neuroscience* 73:657–666.
- Santos RA, Simoes e Silva AC, Maric C, Silva DM, Machado RP, de Buhr I, Heringer-Walther S, Pinheiro SV, Lopes MT, Bader M, Mendes EP, Lemos VS, Campagnole-Santos MJ, Schultheiss HP, Speth R, Walther T (2003) Angiotensin-(1–7) is an endogenous ligand for the G protein-coupled receptor Mas. *Proc Natl Acad Sci U S A* 100:8258–8263.
- Schmidtke A, Tegeder I, Geisslinger G (2009) No NO, no pain? The role of nitric oxide and cGMP in spinal pain processing. *Trends Neurosci* 32:339–346.
- Shimamura M, Kawamuki K, Hazato T (1987) Angiotensin III: a potent inhibitor of enkephalin-degrading enzymes and an analgesic agent. *J Neurochem* 49:536–540.
- Sousa AM, Prado WA (2001) The dual effect of a nitric oxide donor in nociception. *Brain Res* 897:9–19.
- Tamura EK, Cecon E, Monteiro AW, Silva CL, Markus RP (2009) Melatonin inhibits LPS-induced NO production in rat endothelial cells. *J Pineal Res* 46:268–274.
- Tonnaer JA, Wiegant VM, de Jong W, De Wied D (1982) Central effects of angiotensins on drinking and blood pressure: structure–activity relationships. *Brain Res* 236:417–428.
- Vandermeulen EP, Brennan TJ (2000) Alterations in ascending dorsal horn neurons by a surgical incision in the rat foot. *Anesthesiology* 93:1294–1302.
- Villarreal CF, Kina VA, Prado W (2004) Participation of brainstem nuclei in the pronociceptive effect of lesion or neural block of the anterior pretectal nucleus in a rat model of incisional pain. *Neuropharmacology* 47:117–127.
- von Bohlen und Halbach O, Albrecht D (2006) The CNS renin–angiotensin system 6. *Cell Tissue Res* 326:599–616.
- Wilk S (1983) Prolyl endopeptidase. *Life Sci* 33:2149–2157.
- Wright JW, Harding JW (1995) Brain angiotensin receptor subtypes AT1, AT2, and AT4 and their functions. *Regul Pept* 59:269–295.
- Wright JW, Harding JW (2010) The brain RAS and Alzheimer's disease. *Exp Neurol* 223:326–333.
- Yang CH, Shyr MH, Tan PP, Chan SH (1996) Participation of AT1 and AT2 receptors in the differential interaction between angiotensin II or III and alpha-2 adrenoceptors in the nucleus reticularis gigantocellularis in cardiovascular regulation and antinociception in rats. *J Pharmacol Exp Ther* 279:795–802.
- Zhang Q, Fast W, Marletta MA, Martasek P, Silverman RB (1997) Potent and selective inhibition of neuronal nitric oxide synthase by N omega-propyl-L-arginine. *J Med Chem* 40:3869–3870.

(Accepted 21 November 2012)  
(Available online 5 December 2012)